HHS Public Access

Author manuscript

Science. Author manuscript; available in PMC 2017 March 30.

Published in final edited form as:

Science. 2016 June 24; 352(6293): 1542–1547. doi:10.1126/science.aaf5023.

Atomic structure of Hsp90:Cdc37:Cdk4 reveals Hsp90 regulates kinase via dramatic unfolding

Kliment A. Verba[1], **Ray Yu-Ruei Wang**[1], **Akihiko Arakawa**[2], **Yanxin Liu**[1], **Mikako Shirouzu**[2], **Shigeyuki Yokoyama**[2], and **David A. Agard**[1,*]

[1]Howard Hughes Medical Institute and the Department of Biochemistry & Biophysics, University of California San Francisco, San Francisco, CA 94158, USA

[2]RIKEN Systems and Structural Biology Center, 1-7-22 Suehiro-cho, Tsurumi-ku, Yokohama 230-0045, Japan

Abstract

The Hsp90 molecular chaperone and its Cdc37 co-chaperone help stabilize and activate over half of the human kinome. However, neither the mechanism by which these chaperones assist their client kinases nor why some kinases are addicted to Hsp90 while closely related family members are independent is known. Missing has been any structural understanding of these interactions, with no full-length structures of human Hsp90, Cdc37 or either of these proteins with a kinase. Here we report a 3.9Å cryoEM structure of the Hsp90:Cdc37:Cdk4 kinase complex. Cdk4 is in a novel conformation, with its two lobes completely separated. Cdc37 mimics part of the kinase N-lobe, stabilizing an open kinase conformation by wedging itself between the two lobes. Finally, Hsp90 clamps around the unfolded kinase β5 strand and interacts with exposed N- and C-lobe interfaces, protecting the kinase in a trapped unfolded state. Based on this novel structure and extensive previous data, we propose unifying conceptual and mechanistic models of chaperone-kinase interactions.

Main Text

The human kinome is responsible for regulating about a third of all proteins through phosphorylation(1). Proper regulation of this process is important, as misregulated kinase activity can lead to cell death and disease(2). To achieve fine regulation, kinase activity can be sensitively modulated by multiple allosteric inputs. Thus, kinase domains are organized so that dispersed small structural changes caused by binding of regulatory domains/proteins or phosphorylation, can significantly alter kinase activity. Examples of such regulator interactions abound, via SH2/SH3 domains for Src family kinases, dimerization for EGFR or Raf family kinases, and cyclin regulation for Cdks being well characterized examples(3).

*Correspondence to: agard@msg.ucsf.edu.

Supplementary Materials:
Materials and Methods
Figures S1–S13
Tables S1–S2
Movies S1–S4
References (36–57)

Beyond these specific regulators, the Hsp90 molecular chaperone, a member of the general cellular protein folding machinery, also plays a fundamental role in the regulation of many kinases(4). While usually chaperones facilitate the early steps of protein folding, Hsp90 also functions late in the folding process to help both fold and activate a set of protein "clients" (~10% of the proteome)(5). Notably ~60% of the human kinome interacts with Hsp90 with the assistance of its kinase specific cochaperone Cdc37(6). Pharmocologic inhibition of Hsp90 leads to rapid ubiquitinylation and degradation of client kinases. As many Hsp90/Cdc37-dependent kinases are key oncoproteins, (vSrc, bRafV600E, Her2, etc.) several Hsp90 inhibitors are undergoing clinical trials as cancer therapeutics(7).

Hsp90 is a well conserved, but highly dynamic molecular machine. Each monomer within the Hsp90 dimer has three structural domains: a C-terminal domain (CTD) responsible for dimerization; a middle domain (MD) implicated in client binding; and the N-terminal domain (NTD) that binds ATP. Without bound nucleotide, Hsp90 mostly populates a variety of "open" states, whereas nucleotide binding promotes formation of a closed state in which the NTDs also dimerize, followed by hydrolysis(8, 9). The rates of closure and hydrolysis are homologue specific, with human cytosolic Hsp90s almost always open, while yeast Hsp90 preferentially adopts a fully closed state (10). Towards the end of the NTD is a highly charged region ("charged linker") that shows wide variation in length and composition between species. The function and the structure of the charged linker are unclear, but deletion can impact Hsp90 function(11).

Cdc37 is less well studied. The monomeric protein can also be divided into three domains: an N-terminal domain of unknown structure that interacts with kinases, a globular middle domain which interacts with Hsp90 and an extended C terminal domain, of unknown function(12). Although there is a cocrystal structure of the Cdc37 middle/C domains (Cdc37 M/C) bound to the Hsp90-NTD(13), there is evidence that Cdc37 may also interact with the MD of Hsp90(14). Phosphorylation of Cdc37 serine 13 plays an important role, providing stabilizing interactions *in vitro*(15) and being functionally necessary *in vivo*(16).

Although there is a wealth of *in vivo* data, a physical understanding of how Hsp90 and Cdc37 facilitate kinase function is lacking. Equally unclear is why some kinases are strongly Hsp90-dependent whereas closely related kinases are Hsp90-independent. Despite numerous attempts to identify a consistent motif responsible for Hsp90 interaction, the only general trend that has emerged is that client kinases appear to be less thermally stable than non-clients(6). In support of this, binding of kinase inhibitors or allosteric regulators reduce Hsp90 interactions(17, 18). While reasonable that less stable kinases might depend on Hsp90, it remains unclear why this happens or what Hsp90 recognizes. Despite its obvious value, obtaining a crystal structure of an Hsp90:Cdc37:kinase complex has been unsuccessful due to the dynamic nature of Hsp90-client interactions, and challenges in reconstituting the complex. Encouraged by previous negative stain EM studies(19) and the recent advances in cryoEM detectors and processing methodologies that together make analysis of such a small, asymmetric complex feasible(20), we undertook cryoEM studies of the human 240KDa Hsp90:Cdc37:Cdk4 kinase complex.

Complex formation and cryoEM structural analysis

Human homologues of all three proteins were co-expressed in Sf9 insect cells. A stable ternary complex that survived rigorous dual-tag purification formed in the presence of molybdate (Fig S1). Although the mode of molybdate action is unknown, it affects Hsp90's hydrolysis rate and helps stabilize Hsp90-client interactions(21). Simply mixing components individually purified from insect cells did not yield any detectable complex; therefore either post translational modifications specific to the complex or other components (like Hsp40/Hsp70) are required. Despite significant effort to optimize conditions and image processing, preferential particle orientation and conformational heterogeneity limited initial reconstructions from data collected in house to about 6–8Å resolution. To move forward a much larger data set was collected at National Resource for Automated Molecular Microscopy (NRAMM)(22). Data quality was verified as 2D classification of ~800,000 initially picked particles yielded classes with visible high-resolution features (Fig S2). 3D classification and refinement resulted in a 4Å map (Fig S3, S4 and Table S1), with most of Hsp90 being better resolved (3.5Å), while the lowest resolution regions were around 6Å (Fig 1A).

Hsp90 is in a closed conformation in the complex

Refining the 4Å map with a tighter mask around Hsp90 generated a higher resolution, 3.9Å density for Hsp90 and neighboring regions (Fig. 1B inserts)(22). This map was of sufficient quality to accurately build and refine an atomic model of human Hsp90β based on a homology model derived from yeast Hsp90 (Fig 1B and S5). Surprisingly, reconstructions of complex prepared with Hsp90 with deleted charged linker never yielded good results, likely due to increased heterogeneity. Hsp90 adopts a symmetrical (RMSD between monomers=0.82Å), closed conformation, closely resembling the yHsp90 closed state(23). This was unexpected, as without crosslinker, closed hHsp90 had not previously been observed. While the molybdate added during purification may contribute, the closed state is likely a consequence of the ternary complex. In our map, which was refined without symmetry, the strongest density is symmetric at the γ-phosphate location for nucleotide binding sites at both NTDs of Hsp90 (Fig S6). This suggests that either the complex traps Hsp90 in an ATP state, or, more likely, ADP-molybdate acts as a post hydrolysis transition state inhibitor, thereby helping stabilize the closed conformation. The hHsp90 model determined here is similar to the yeast Hsp90 (RMSD=1.59Å), with a small rotation in the CTD and correlated movements throughout (Movie S1). Additionally, a number of loops disordered in the crystal structure were ordered in our model, as they were interacting with the kinase. (Fig 2B) The charged linker is visible in 2D classes, but absent from the 3D reconstruction, suggesting a highly flexible structure (Fig S2).

The N-lobe of Cdk4 is significantly unfolded and threads through Hsp90

Two regions of the 4Å map cannot be accounted for by Hsp90: a long coiled-coil like protrusion and a globular density on one side of Hsp90 (arrows, Fig 1B). While we initially suspected that these corresponded to the Cdc37M/C (globular domain with long helix), as our map improved the globular domain fit became worse. To obtain an unbiased fit, an

exhaustive search was performed against all protein folds in the CATH database (~16000 PDBs) (22). Disregarding algorithmic errors, the top scoring hits were all variations on the kinase C-lobe, with Cdc37M/C scoring considerably worse (Fig S7). Based on this, the Cdk4 C-lobe was placed into the density(24), resulting in a high quality fit (Fig 2A). By contrast, not only no suitable density exists for the folded kinase N-lobe but it would sterically clash with Hsp90. Remarkably, tracing the kinase density from the C-lobe towards the N-terminus, there was a clear tubular region going through the lumen of Hsp90 (Fig 2A, 2B). Thus, a drastically altered conformation of the kinase N-lobe is being stabilized by Hsp90. (Movie S2) Threading the Cdk4 sequence into this density, reveals that β4 and β5 strands have been ripped apart and instead β5 interacts with a previously mapped general Hsp90 client binding site via extensive hydrophobic interactions(25) and two salt bridges (Fig 2C). Potentially due to these interactions, there is a rotation of Hsp90 CTD towards the kinase (as compared to yHsp90 structure) at the MD:CTD interface, which was identified as asymmetric in previous work(26) (Movie S1). Altogether this suggests that the MD:CTD interface may be used to communicate Hsp90's hydrolysis state to the client. Unfortunately, in the highest resolution map no density was visible for kinase residues N-terminal of the β5 strand.

Cdc37 is split into two domains and wraps around Hsp90

While there is no available 3D structural information for the Cdc37 N-terminal domain, sequence analysis (MARCOIL) predicts significant coiled coil structure. Supported by our observations of high helical content by CD and NMR (Fig S8), this provides a good candidate for the non-globular map density (Fig 1B). That density, transitions from helical to strand like, wrapping around the Hsp90MD and adding an additional β-strand to the 1AC β-sheet (2CG9 nomenclature). Unfortunately, as with the kinase, this β-strand does not connect to any density on the other side, thwarting a complete fit of Cdc37. Showing the power of single particle cryoEM, local rounds of 3D classification yielded a 7Å map (Fig S3, S9) showing clear globular density that connected through the β-strand to the coiled-coil region (Fig 3A). This new density was unambiguously fit by the crystallized Cdc37M/C fragment. Using a combination of the two maps, we were able to fit Cdc37M/C residues 148–260 and de-novo build residues 1–147 of human Cdc37 (Fig 3A) (22). Although further classification revealed some density beyond residue 260, it was too weak to model with confidence.

Locating the remainder of the kinase N-lobe and verification

The local 3D classification also revealed the remainder of the kinase N-lobe (Fig 3B and Movie S3). In two of the classes, distinct globular densities were visible that connected to the tubular density derived from the unfolded Cdk4 N-lobe. At the same time, the density for the middle domain of Cdc37 was either very weak or absent, suggesting an anti-correlation between Cdc37M/C:Hsp90 interactions and kinase N-lobe:Hsp90 interactions. We were able to roughly fit the rest of the Cdk4 N-lobe into these densities, allowing us to build a complete model of Hsp90:Cdc37:Cdk4 complex (Fig 4 and Movie S4). Given the unusual split domain conformation for both the kinase and cochaperone, it was important to verify our structural assignments. Towards that end, we covalently tagged Cdc37 at its N terminus

and Cdk4 at its C terminus with T4 lysozyme. The two different complexes were expressed and purified from yeast, followed by cryoEM reconstruction of each. These two structures clearly show lysozyme density consistent with our map interpretation (Fig S10).

Cdc37 precisely mimics a conserved feature of kinase N-lobe-C-lobe interactions and makes novel interactions with Hsp90

There are a number of striking features from the resulting model (Fig 4) that explain a wealth of accumulated, seemingly contradictory observations. The Cdc37NTD forms a long coiled-coil with a leucine zipper like motif. The N-terminus of this coiled-coil interacts with Cdk4 through extensive hydrophobic and hydrogen bonding interactions, burying 725 $Å^2$ (Table S2) in surface area, and mimicking interactions that the kinase αC-β4 loop normally makes with the C-lobe (Fig 5A). More strikingly, the following loop in Cdc37, overlays perfectly with the αC-β4 loop of multiple kinases, packing tightly against the kinase C lobe (Fig 5A, bottom insert), explaining why this Cdc37 region is so conserved (Fig. S11). Thus Cdc37 binds to the kinase C-lobe by mimicking interactions the N-lobe would normally have made, stabilizing separation of the two kinase lobes.

The interactions between Cdc37 and Hsp90 are significantly different from those seen in the previous crystal structure of fragments of each protein. Instead of binding to an Hsp90NTD surface that would only be accessible in the open state, in the Hsp90 closed state, Cdc37M/C interacts with Hsp90MD, although these interactions are fairly limited (only about 340$Å^2$ out of 2650$Å^2$ total buried surface area) (Fig 4). More extensive are interactions from Cdc37 residues 120–129, which pack a β-strand against Hsp90 MD (Fig 5B). Additionally part of the Cdc37NTD binds to a new site on the closed Hsp90NTD, somewhat mimicking interactions seen between p23 and Hsp90 (Fig 5B, top insert). There is also a network of ionic interactions between Cdc37NTD and Hsp90MD, which explains previously identified salt sensitivity of Cdc37/Hsp90 binding (Fig 5B, bottom insert). Our structure thus helps explain recent data that *C. elegans* Cdc37 interacts with the middle domain of Hsp90(27), rather than the NTD as observed in previous human domain binding studies. Instead of assuming that *C. elegans* is different or that the interactions observed with isolated domains were incorrect, we propose that Cdc37/kinase first binds Hsp90 in its open conformation as seen in the crystal structure, and then rearranges to the site on the middle domain upon Hsp90 closure, as seen in our structure.

Phosphorylation of Cdc37 stabilizes kinase bound conformation

Phosphorylation at the completely conserved Cdc37:S13 is important for kinases to function, and was thought to be directly involved in kinase binding (15,16). In our structure there is density for the phosphorylated-serine13, which forms a salt bridge with Cdc37:R36 and Cdc37:H33, stabilizing the very N-terminus of the coiled coil (Fig 5B middle insert). This provides a molecular rationale for previous observations of a Cdc37 conformational change upon phosphorylation(28). Of note, this phosphate also contributes to the overall electrostatic nature of Hsp90-Cdc37 interactions, forming a salt bridge with Hsp90:K406.

The residues comprising Cdc37/Hsp90NTD and Cdc37/kinase interaction surfaces are extremely well conserved (Fig S11), further validating the significance of the interactions observed here.

Hsp90/Cdc37 capture and stabilize structural transitions within the kinase

In ternary complex, Cdk4 assumes a conformation drastically different than previously seen for any kinase structure. The kinase hinge region and β4-β5 sheets are completely unfolded, with the N lobe and C lobe being pried apart and stabilized by new interactions with Hsp90 and Cdc37. Based on this, we propose a model where it is not a specific binding sequence, but the propensity for the kinase to unfold to a N-lobe/C-lobe separated open state, that determines whether a particular kinase will be a client. Furthermore, the fact that many non-client kinases depend on Hsp90 during initial folding would suggest that the open kinase state we observe is an on pathway folding intermediate.

In agreement with the model, the β3-αC loop of Cdk4 (strong client) has seven glycines versus one/two glycines in the same loop of Cdk2 and Cdk6 (non client and weak client respectively). Mutating this loop in Cdk4 to the Cdk6 sequence stabilizes the protein(29). In a similar manner, a single point mutation derived from EGFR (non-client) in the αC-β4 loop was able to abrogate the interactions of HER2 (strong client) with, and dependence on, Hsp90/Cdc37(30). This point mutation would potentially introduce a salt bridge stabilizing the kinase loop (Fig S12), and hence the association between the kinase lobes.

Our model explains why a sequence motif responsible for Hsp90 interactions has yet to be found. The remarkable allostery of kinases allows distant and seemingly un-related mutations to destabilize the N-lobe/C-lobe interface explaining often confusing mutagenesis results. Thus non-client kinases would exit Hsp90 dependence after initial folding via stabilizing interactions with regulatory partners/extra domains (cyclin, dimerization partners, SH2/SH3 domains, etc.)

Linking kinase unfolding to assembly and activity

Why might it be beneficial for a large percentage of human kinases to significantly populate a folding intermediate even when mature? Rather than being a vestige of kinase evolution with Hsp90 buffering gain of function destabilizing mutations (31), we argue that being able to safely populate such an open folding intermediate has a direct functional/regulatory benefit. Recent computational efforts have suggested a connection between folding and kinase activity(32, 33). The concept is that the most favorable transition between the inactive and active states is through a more open, unfolded state rather than through a more classical rigid-body transition. Although the opening seen in simulations is far more subtle than that observed here, we suggest that the concept still applies (Fig 6A). The generally lower stability of client kinases would lead to enhanced sampling of the open state, thereby encouraging chaperone binding (Fig 6B). Chaperone stabilization of a kinase open state could increase the overall rates of interconversion and/or protect a potentially vulnerable state from aggregation or recognition by the ubiquitinylation machinery. Moreover, the open

state could be the preferred substrate for adding/removing post-translational modifications as well as for critical stabilizing interactions.

Life cycle of kinase:Hsp90:Cdc37 interactions

Our structure also suggests how the observed state might arise and mature (Fig 6C). Hsp90 would first interact with Cdc37/kinase via previously published crystal structure contacts (Fig 6C, state III). Whether assistance from Hsp70/Hsp40 as with the glucocorticoid receptor would be required is as yet unclear(34), but the inability to directly form the complex from components and Chk1 reconstitution experiments(35) are suggestive. During the cycle, Cdc37 would act as a quality control checkpoint, where only upon proper folding of the N-lobe would it dissociate from the kinase. Long coiled-coil would allow Cdc37/kinase to stay attached to Hsp90 during multiple ATP hydrolysis events. If the kinase would fail to dissociate after many hydrolysis events, the degradation machinery might then be recruited to the complex. While Fig 6C captures the essence of the available data, other models are possible.

Beyond revealing the kinase open state, our cryo EM reconstruction allowed us to build first atomic models for the human cytosolic Hsp90 and the kinase interacting N terminus of Cdc37. The ability to collect a large number of particles coupled with the capabilities of single electron counting detectors and 3D classification software, allowed us to visualize multiple conformations, providing a qualitative assessment for the dynamic nature of the complex. Overall, our structure has explained a number of often contradictory, biochemical observations and provided both mechanistic and conceptual models of Hsp90:kinase interactions, that can be tested in future experiments. It also indicates the potential of single particle cryoEM for exploring other challenging dynamic, asymmetric complexes at near atomic resolution.

Supplementary Material

Refer to Web version on PubMed Central for supplementary material.

Acknowledgments

We thank members of NRAMM-Scripps for help with collecting data, Yao Fan for the yeast expression vector, Naomi Ohbayashi and Mutsuko Niino (RIKEN Center for Life Science Technologies) for help with Sf9 protein expression, Dr. Neil F Rebbe (The University of North Carolina at Chapel Hill) and Dr. Ernest Laue (The University of Cambridge) for the plasmids encoding human HSP90b and Cdc37, respectively, D.A.A. lab members for helpful discussions and Natalia Jura for reading the manuscript. Support for this work was provided by PSI-Biology grant U01 GM098254 (to D.A.A.), AACR-BCRF Grant 218084 for Translational Breast Cancer Research (to D.A.A.), The Cabala Family gift (to D.A.A.), HHMI Helen Hay Whitney Foundation Fellowship (to Y.L.), HHMI International Student Research Fellowship (to K.V.) and the Howard Hughes Medical Institute (to D.A.A.). Some of the work presented here was conducted at NRAMM, which is supported by a grant from the National Institute of General Medical Sciences (9 P41 GM103310) from the National Institutes of Health. Some of the work used the Extreme Science and Engineering Discovery Environment (XSEDE), which is supported by National Science Foundation grant number ACI-1053575.

References and notes

1. Taylor SS, Keshwani MM, Steichen JM, Kornev AP. Evolution of the eukaryotic protein kinases as dynamic molecular switches. Philos Trans R Soc Lond B Biol Sci. 2012; 367:2517–2528. [PubMed: 22889904]
2. Zhang J, Yang PL, Gray NS. Targeting cancer with small molecule kinase inhibitors. Nat Rev Cancer. 2009; 9:28–39. [PubMed: 19104514]
3. Endicott JA, Noble ME, Johnson LN. The structural basis for control of eukaryotic protein kinases. Annu Rev Biochem. 2012; 81:587–613. [PubMed: 22482904]
4. Brugge J, Yonemoto W, Darrow D. Interaction between the Rous sarcoma virus transforming protein and two cellular phosphoproteins: analysis of the turnover and distribution of this complex. Mol Cell Biol. 1983; 3:9–19. [PubMed: 6298609]
5. Taipale M, Jarosz DF, Lindquist S. HSP90 at the hub of protein homeostasis: emerging mechanistic insights. Nat Rev Mol Cell Biol. 2010; 11:515–528. [PubMed: 20531426]
6. Taipale M, et al. Quantitative analysis of HSP90-client interactions reveals principles of substrate recognition. Cell. 2012; 150:987–1001. [PubMed: 22939624]
7. Miyata Y, Nakamoto H, Neckers L. The therapeutic target Hsp90 and cancer hallmarks. Curr Pharm Des. 2013; 19:347–365. [PubMed: 22920906]
8. Krukenberg KA, Street TO, Lavery LA, Agard DA. Conformational dynamics of the molecular chaperone Hsp90. Q Rev Biophys. 2011; 44:229–255. [PubMed: 21414251]
9. Mayer MP, Le Breton L. Hsp90: breaking the symmetry. Mol Cell. 2015; 58:8–20. [PubMed: 25839432]
10. Southworth DR, Agard DA. Species-dependent ensembles of conserved conformational states define the Hsp90 chaperone ATPase cycle. Mol Cell. 2008; 32:631–640. [PubMed: 19061638]
11. Tsutsumi S, et al. Charged linker sequence modulates eukaryotic heat shock protein 90 (Hsp90) chaperone activity. Proc Natl Acad Sci U S A. 2012; 109:2937–2942. [PubMed: 22315411]
12. Shao J, Irwin A, Hartson SD, Matts RL. Functional dissection of cdc37: characterization of domain structure and amino acid residues critical for protein kinase binding. Biochemistry. 2003; 42:12577–12588. [PubMed: 14580204]
13. Roe SM, et al. The Mechanism of Hsp90 regulation by the protein kinase-specific cochaperone p50(cdc37). Cell. 2004; 116:87–98. [PubMed: 14718169]
14. Eckl JM, et al. Cdc37 (cell division cycle 37) restricts Hsp90 (heat shock protein 90) motility by interaction with N-terminal and middle domain binding sites. J Biol Chem. 2013; 288:16032–16042. [PubMed: 23569206]
15. Polier S, et al. ATP-competitive inhibitors block protein kinase recruitment to the Hsp90-Cdc37 system. Nat Chem Biol. 2013; 9:307–312. [PubMed: 23502424]
16. Vaughan CK, et al. Hsp90-dependent activation of protein kinases is regulated by chaperone-targeted dephosphorylation of Cdc37. Mol Cell. 2008; 31:886–895. [PubMed: 18922470]
17. Taipale M, et al. Chaperones as thermodynamic sensors of drug-target interactions reveal kinase inhibitor specificities in living cells. Nat Biotechnol. 2013; 31:630–637. [PubMed: 23811600]
18. Boczek EE, et al. Conformational processing of oncogenic v-Src kinase by the molecular chaperone Hsp90. Proc Natl Acad Sci U S A. 2015; 112:E3189–3198. [PubMed: 26056257]
19. Vaughan CK, et al. Structure of an Hsp90-Cdc37-Cdk4 complex. Mol Cell. 2006; 23:697–707. [PubMed: 16949366]
20. Cheng Y. Single-Particle Cryo-EM at Crystallographic Resolution. Cell. 2015; 161:450–457. [PubMed: 25910205]
21. Hartson SD, Thulasiraman V, Huang W, Whitesell L, Matts RL. Molybdate inhibits hsp90, induces structural changes in its C-terminal domain, and alters its interactions with substrates. Biochemistry. 1999; 38:3837–3849. [PubMed: 10090774]
22. Materials and methods are available as supplementary materials at the Science website.
23. Ali MM, et al. Crystal structure of an Hsp90-nucleotide-p23/Sba1 closed chaperone complex. Nature. 2006; 440:1013–1017. [PubMed: 16625188]

24. Takaki T, et al. The structure of CDK4/cyclin D3 has implications for models of CDK activation. Proc Natl Acad Sci U S A. 2009; 106:4171–4176. [PubMed: 19237555]
25. Genest O, et al. Uncovering a region of heat shock protein 90 important for client binding in E. coli and chaperone function in yeast. Mol Cell. 2013; 49:464–473. [PubMed: 23260660]
26. Lavery LA, et al. Structural asymmetry in the closed state of mitochondrial Hsp90 (TRAP1) supports a two-step ATP hydrolysis mechanism. Mol Cell. 2014; 53:330–343. [PubMed: 24462206]
27. Eckl JM, et al. Hsp90.Cdc37 Complexes with Protein Kinases Form Cooperatively with Multiple Distinct Interaction Sites. J Biol Chem. 2015; 290:30843–30854. [PubMed: 26511315]
28. Liu W, Landgraf R. Phosphorylated and unphosphorylated serine 13 of CDC37 stabilize distinct interactions between its client and HSP90 binding domains. Biochemistry. 2015; 54:1493–1504. [PubMed: 25619116]
29. Day PJ, et al. Crystal structure of human CDK4 in complex with a D-type cyclin. Proc Natl Acad Sci U S A. 2009; 106:4166–4170. [PubMed: 19237565]
30. Xu W, et al. Surface charge and hydrophobicity determine ErbB2 binding to the Hsp90 chaperone complex. Nat Struct Mol Biol. 2005; 12:120–126. [PubMed: 15643424]
31. Lachowiec J, Lemus T, Borenstein E, Queitsch C. Hsp90 promotes kinase evolution. Mol Biol Evol. 2015; 32:91–99. [PubMed: 25246701]
32. Miyashita O, Onuchic JN, Wolynes PG. Nonlinear elasticity, proteinquakes, and the energy landscapes of functional transitions in proteins. Proc Natl Acad Sci U S A. 2003; 100:12570–12575. [PubMed: 14566052]
33. Shan Y, Arkhipov A, Kim ET, Pan AC, Shaw DE. Transitions to catalytically inactive conformations in EGFR kinase. Proc Natl Acad Sci U S A. 2013; 110:7270–7275. [PubMed: 23576739]
34. Kirschke E, Goswami D, Southworth D, Griffin PR, Agard DA. Glucocorticoid receptor function regulated by coordinated action of the Hsp90 and Hsp70 chaperone cycles. Cell. 2014; 157:1685–1697. [PubMed: 24949977]
35. Arlander SJ, et al. Chaperoning checkpoint kinase 1 (Chk1), an Hsp90 client, with purified chaperones. J Biol Chem. 2006; 281:2989–2998. [PubMed: 16330544]

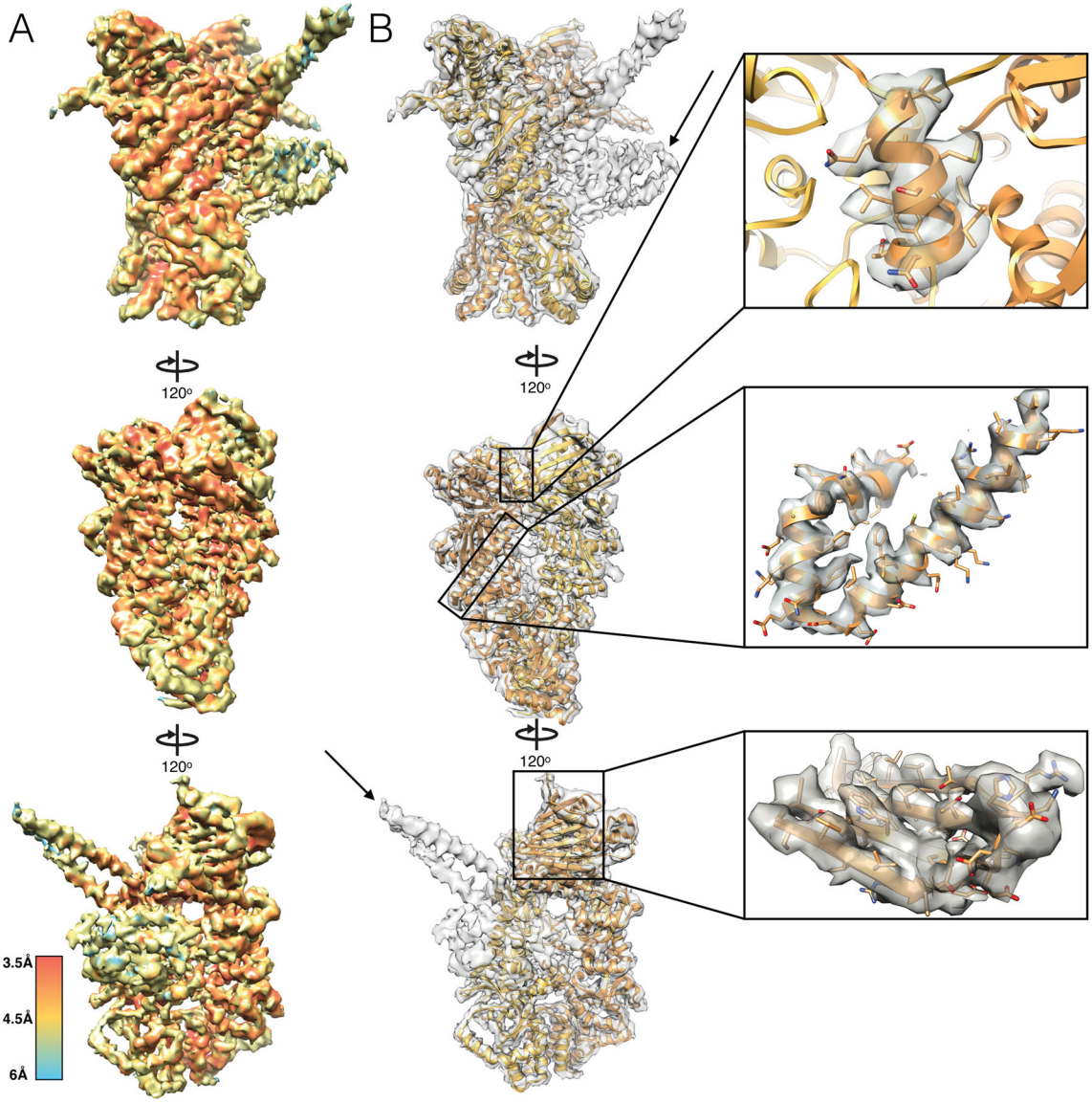

Fig. 1. The 4Å map of Hsp90/Cdc37/Cdk4

Density map colored by resolution. (B) hHsp90β model built into the density map, with different monomers colored shades of orange. Inserts show high resolution features. Arrows show density un-accounted for by Hsp90.

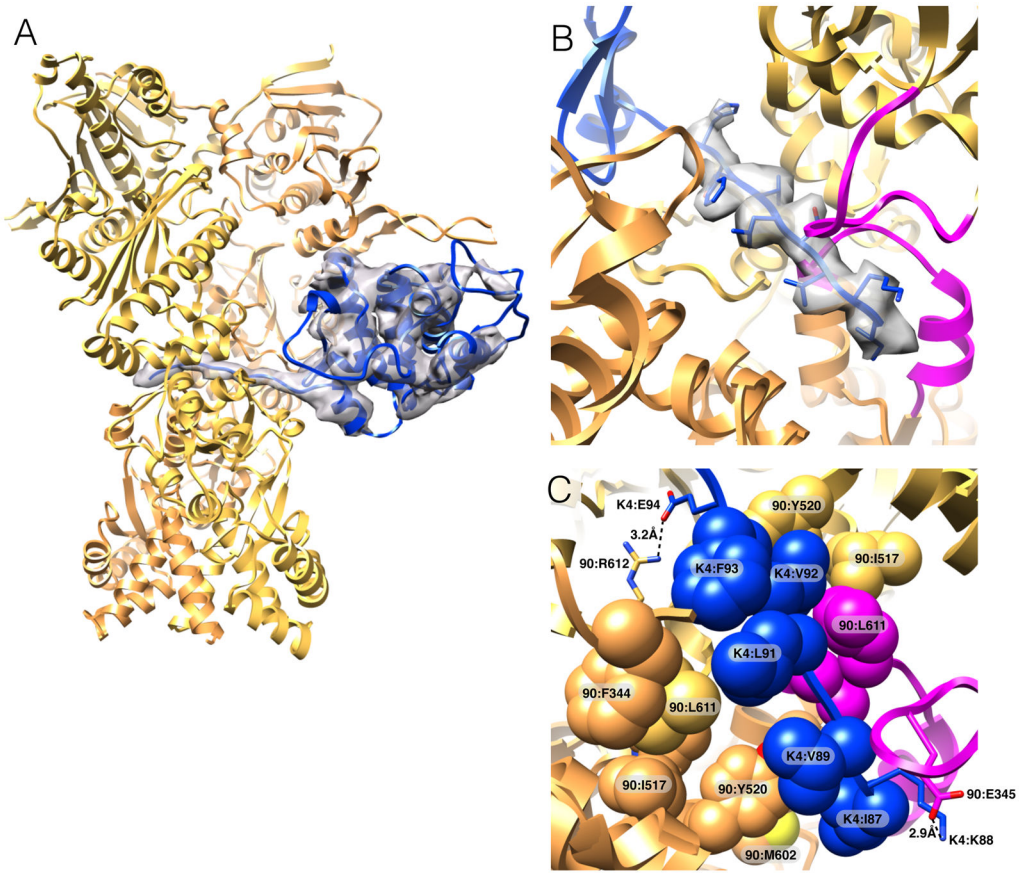

Fig. 2. Cdk4 is unfolded when complexed with Hsp90 and Cdc37

(A) Cdk4 (K4) C-lobe (blue) fit into the map (B) The tubular density from high-resolution map through the lumen of Hsp90 is perfectly fit by an unfolded β5 sheet (in sticks) of Cdk4. In magenta are previously disordered client interacting loops on Hsp90. (C) Cdk4/Hsp90 interface with hydrophobic residues in spheres, salt bridges in sticks.

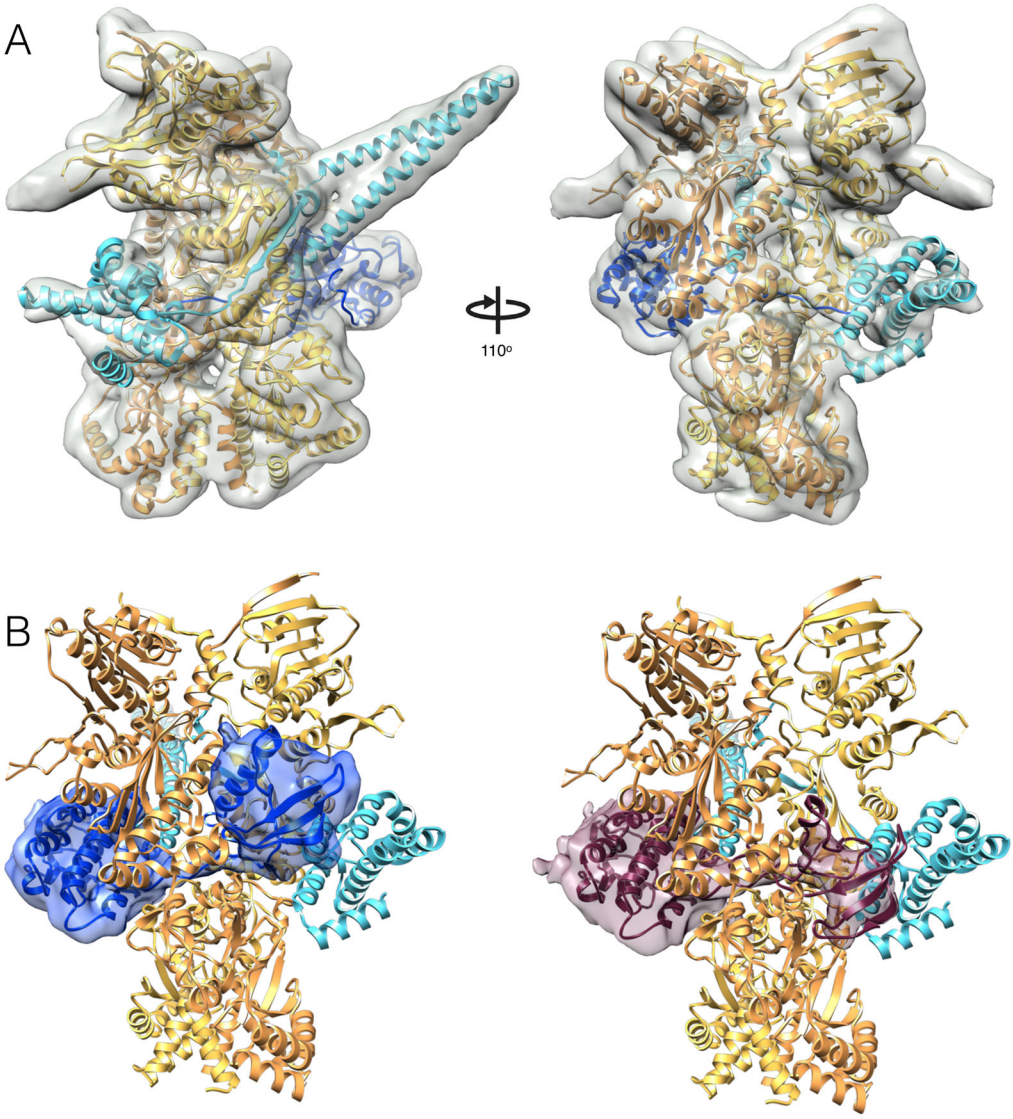

Fig. 3. Rounds of focused 3D classification yield distinct densities for Cdc37 and the Cdk4 N-lobe

One of the new classes has clear density for the Cdc37 (37) M/C fragment crystal structure. In teal is our complete Cdc37 model (residues 1–260). Note the β-strand wrapping around the outside of Hsp90 connecting the two major Cdc37 domains. (B) Two additional classes show new density for the missing Cdk4 N-lobe. The classes minus the Hsp90/Cdc37 density, in blue and maroon, highlight the two new Cdk4 N lobe conformations. Fitted kinase models are in ribbons.

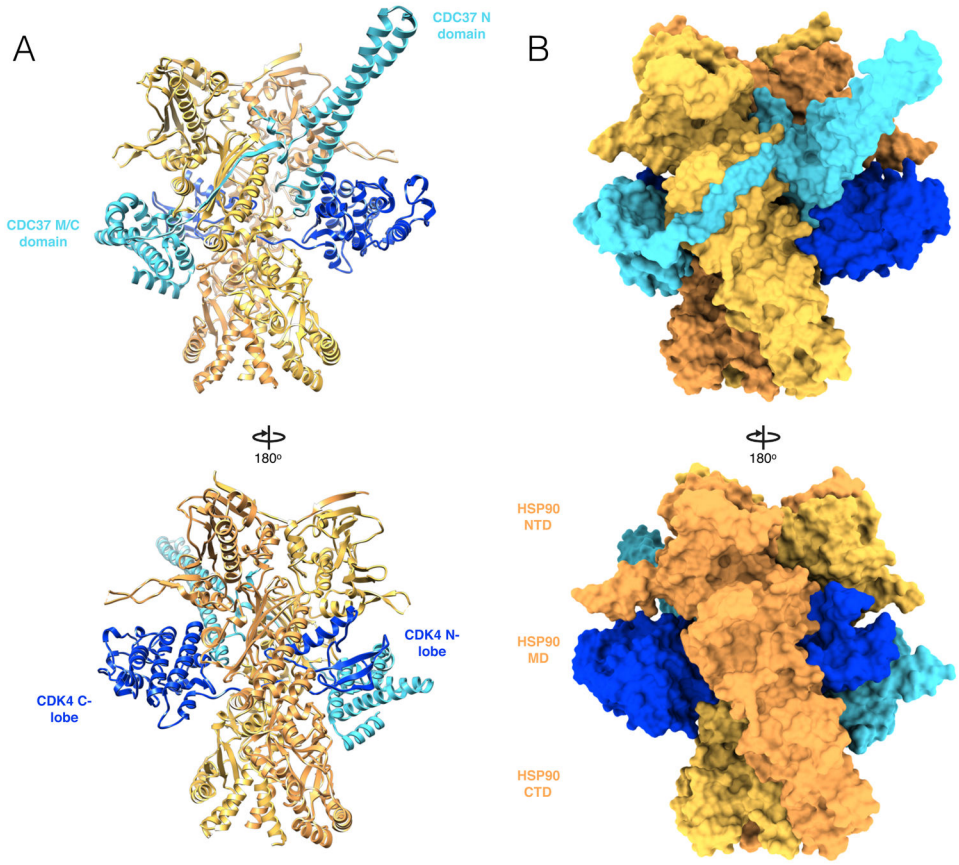

Fig. 4. Hsp90, Cdc37, and Cdk4 are intricately interwoven in the complex

Two views of the complete model, showing ribbon in (A) and surface in (B)

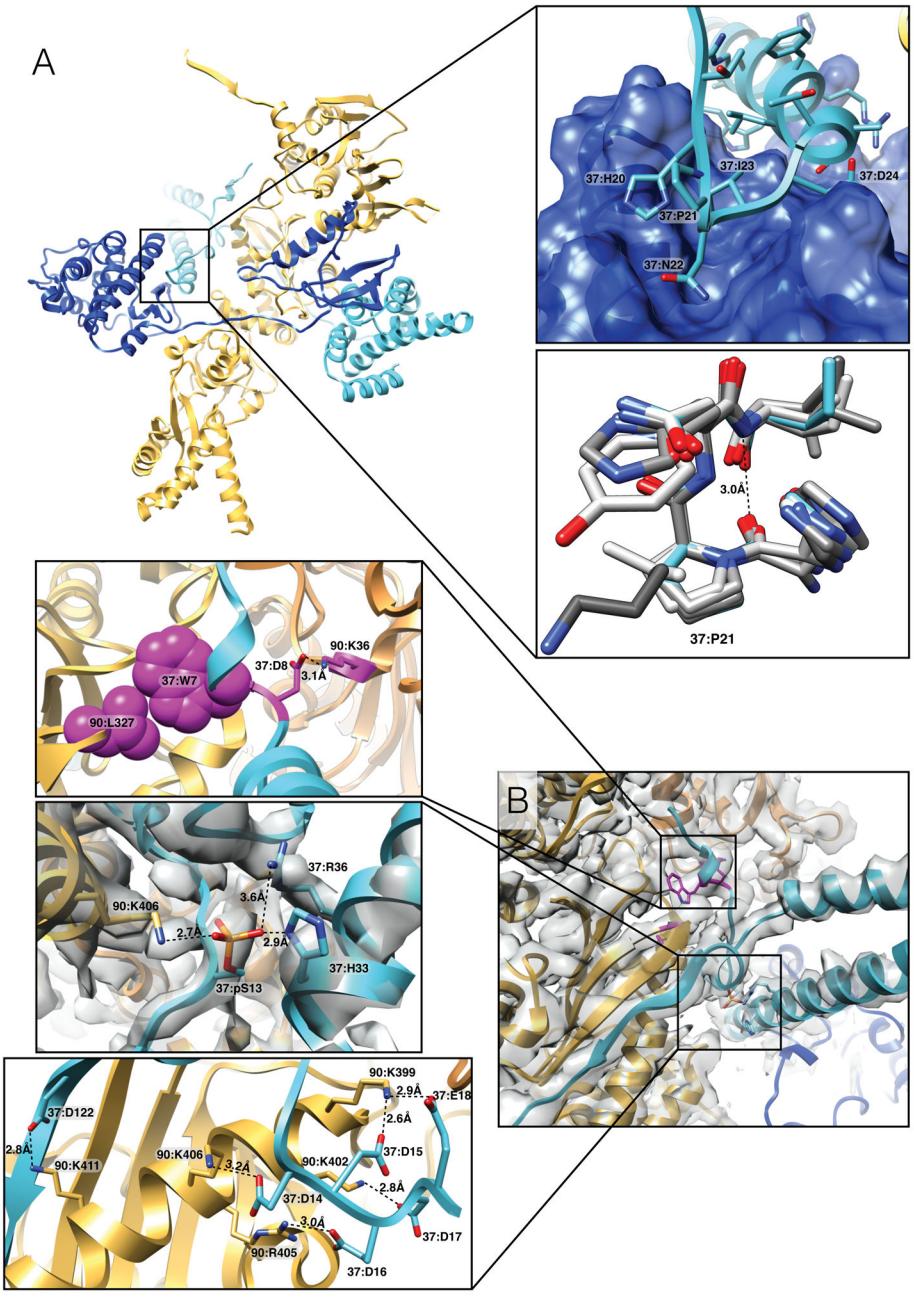

Fig. 5. High-resolution details of Cdc37 interactions with Hsp90 and Cdk4

Overall arrangement of Hsp90/Cdc37/Cdk4 (one Hsp90 monomer removed for clarity). The insets highlight Cdc37/Cdk4 interaction features: top – Cdc37/Cdk4 interact via hydrophobic interactions and backbone hydrogen bonds, with perfect shape complementarity, bottom - overlay of Cdc37's conserved HPN motif (teal) perfectly mimicking type I β-turn of αC-β4 loop of 6 different kinases (shades of gray). (PDB codes: 3g33, 2itp, 1qmz, 3pp0, 1jnk, 4fk3) (B) Zooming in on Hsp90/Cdc37 interactions. Top insert: Cdc37/Hsp90 interactions mimic p23/Hsp90 interactions identified previously (magenta). Middle insert: phospho-Ser13 stabilizes local Cdc37 structure through

interactions with conserved R36 and H33 and also interacts with Hsp90 at K406. Bottom insert: six salt bridges stabilizing Hsp90/Cdc37 interactions.

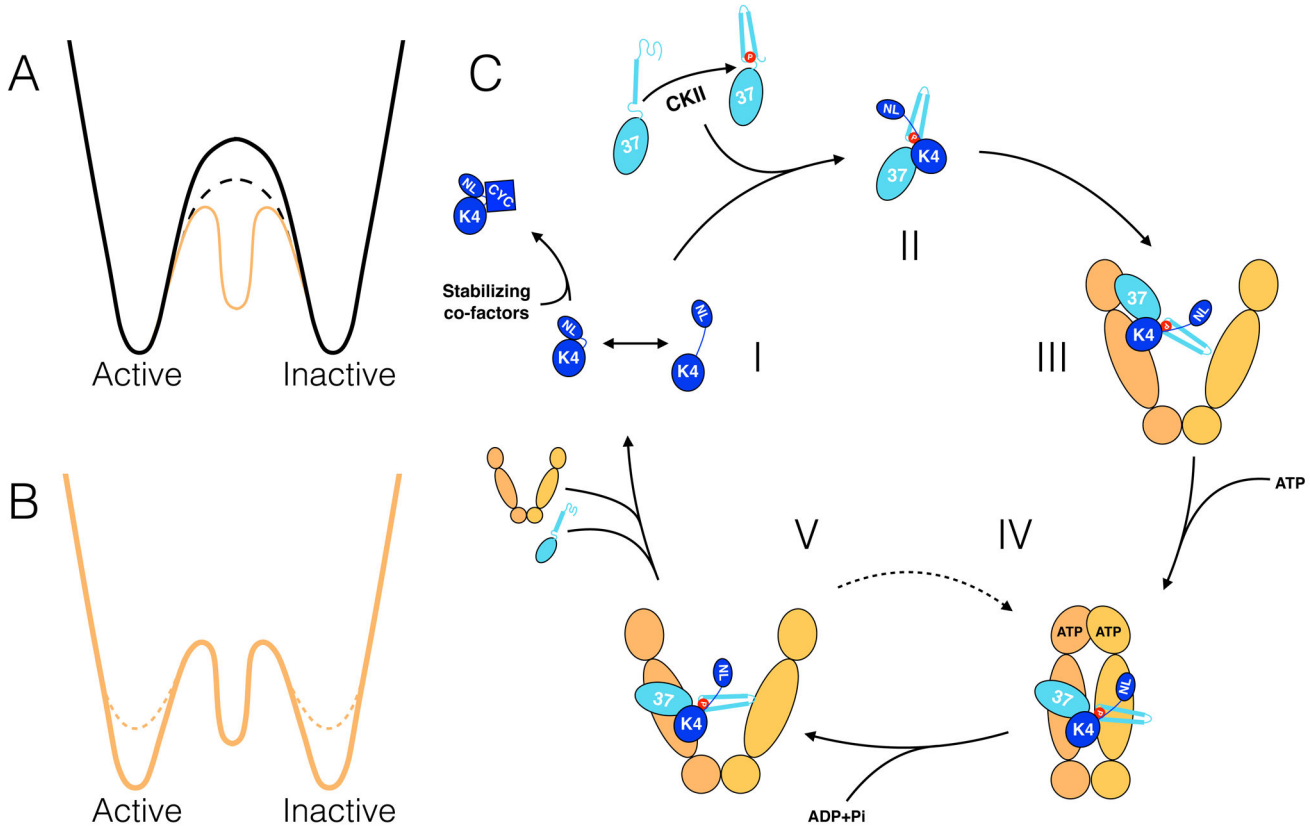

Fig. 6. Conceptual model for linkage between kinase folding and activation and proposed model for the Hsp90:Cdc37:kinase cycle

(A) Transitioning between states through an unfolded intermediate (dashed line) has a lower energy barrier than through rigid body motion (solid line). The Hsp90:Cdc37 stabilizes such an unfolded intermediate (orange solid line) (B). By comparison with non-clients (solid line), the active and inactive states of client kinases (dashed line) are de-stabilized. (C) Speculative model for an Hsp90:Cdc37:Kinase cycle. (I) The kinase domain transiently samples an open state. Interactions with co-factors (like cyclins, SH2/SH3 domains, etc.) stabilizes the kinase native state, disfavoring the open state. (NL-N-lobe, CYC-Cyclin) CKII phosphorylated Cdc37 captures the open state by binding the kinase C-lobe (II). Cdc37/kinase then binds to open Hsp90 (III). Hsp90 binds to ATP and closes upon the unfolded part of the kinase. Cdc37 migrates down, resulting in the structure described here (IV). Upon hydrolysis of ATP, Hsp90 opens with Cdc37/Cdk4 still bound, giving a chance for the kinase to fold (V). If it folds, it displaces Cdc37 and leaves the complex. If however it fails to displace Cdc37, then Hsp90 is able to re-bind ATP and go back to state IV, repeating the process. At some point during this cycle, PP5 phosphatase is recruited to the complex to de-phosphorylate Cdc37.